An in situ spectro-electrochemical monitoring of aqueous effects on polymer/metal oxide interfaces

Pletincx, Sven; Mol, Johannes M.C.; Terryn, Herman; Hubin, Annick; Hauffman, Tom

DOI
10.1016/j.jelechem.2019.113311

Publication date
2019

Document Version
Final published version

Published in
Journal of Electroanalytical Chemistry

Citation (APA)
Pletincx, S., Mol, J. M. C., Terryn, H., Hubin, A., & Hauffman, T. (2019). An in situ spectro-electrochemical monitoring of aqueous effects on polymer/metal oxide interfaces. *Journal of Electroanalytical Chemistry*, *848*, Article 113311. https://doi.org/10.1016/j.jelechem.2019.113311

Journal of Electroanalytical Chemistry 848 (2019) 113311

Contents lists available at ScienceDirect

Journal of Electroanalytical Chemistry

journal homepage: www.elsevier.com/locate/jelechem

An *in situ* spectro-electrochemical monitoring of aqueous effects on polymer/metal oxide interfaces

Sven Pletincx[a,*], Johannes M.C. Mol[b], Herman Terryn[a], Annick Hubin[a], Tom Hauffman[a]

[a] Department of Electrochemical and Surface Engineering (SURF), Vrije Universiteit Brussel, Pleinlaan 2, Brussels 1050, Belgium
[b] Department of Materials Science and Engineering, Delft University of Technology, Mekelweg 2, 2628 CD Delft, The Netherlands

ARTICLE INFO

Article history:
Received 15 April 2019
Received in revised form 25 June 2019
Accepted 15 July 2019
Available online 22 July 2019

Keywords:
Odd random phase multisine electrochemical impedance spectroscopy
ATR-FTIR Kretschmann
Buried interface
Polymer/metal oxide
In situ

ABSTRACT

A spectro-electrochemical setup of Fourier transform infrared spectroscopy (FTIR) in the Kretschmann geometry and odd random phase multisine electrochemical impedance spectroscopy (ORP EIS) is applied to *in situ* monitor the effect of an aqueous electrolyte on the polymer/metal oxide interface. The interfacial interactions of an ultrathin polyacrylic acid (PAA) film on an aluminum oxide surface are identified as carboxylate ionic bonds and changes induced by the effect of water diffusion at the interface are monitored *in situ*. Initially after electrolyte exposure, an increase in ionic bonding is observed. However, eventually the interfacial interactions are replaced by water molecules, leading to macroscopic delamination. By comparing a variation of oxide types, the stability of the interfacial bonds is linked to the amount of free hydroxyl groups on the aluminum oxide surface. An electric equivalent circuit is proposed to model the ORP EIS response of the PAA/aluminum oxide system and the fitted resistance values could be interpreted in a physically meaningful way. Finally, a poly(methyl methacrylate) (PMMA) deposition on aluminum oxide is investigated to explore the effect of a variation in functional groups present at the polymer/metal oxide interface. It is shown that PMMA forms a more stable interface than PAA on native aluminum oxide. This work demonstrates that IR spectroscopy in the Kretschmann geometry and ORP EIS are suited techniques to *in situ* probe interfacial bonds at polymer/metal oxide systems exposed to aqueous conditions. Moreover, a variation of the surface properties of the metal oxide as well as the functional groups of the polymer alter the stability of their mutual interface when exposed to aqueous conditions.

1. Introduction

Corrosion protection of engineering metals against hostile or atmospheric conditions is commonly achieved by covering their top surface with an organic coating. In industry, numerous examples of polymer/(hydr)oxide/metal systems exist. The most straightforward examples are found in infrastructure and in transport (e.g. paints on constructions and protective coatings on all types of transport vehicles). To ensure long service-life, the organic coatings need to withstand long-time exposure to aqueous environments without failing. Unfortunately, the effectiveness of the organic coating against degradation agents is not infinite and eventually the hybrid system will degrade. Macroscopically, this leads to delamination of the organic coating and/or the onset of corrosion of the metal substrate. However, the exact mechanisms leading to coating failure are not yet understood [1].

Monitoring chemical interactions on a local scale at the buried polymer/metal oxide interface is a necessary, but challenging, step in gaining insight in the macroscopic durability of the composite system. The challenging aspect comes from the fact that the interface region is not readily accessible by common (surface) analysis techniques. Their probing depth and/or sensitivity are limited and make it challenging to obtain direct molecular information, which is why this region is often referred to as the buried interface [2]. In order to tackle this accessing problem, the use of a model system and a well-chosen methodology is required to both reach this region, probe information with adequate sensitivity and monitor the effect of external influences *in situ* [3, 4]. Advancements in existing techniques and the development of new experimental approaches enable the possibility to study this region under humid or corrosive conditions [5, 6].

The work reported here is part of an on-going investigation to characterize the interfacial interactions between acrylic polymers and aluminum oxide surfaces [7, 8]. Access to the interface region is achieved by a specific methodology where a thin-film deposition is used. The polymer film is made sufficiently thin, making it possible

* Corresponding author.
E-mail address: Sven.Pletincx@vub.be (S. Pletincx).

https://doi.org/10.1016/j.jelechem.2019.113311
1572-6657/

to study the interaction of functional groups on metal (hydr)oxide surfaces by surface analysis techniques. The deposition of this thin film is achieved by reactive adsorption from a highly diluted polymer solution, leading to organic films with a thickness of the order of nanometers [9-11].

Leadley et al. applied this thin-film approach in combination with X-ray photoelectron spectroscopy (XPS) to study the interface of ultrathin acrylic polymer films on metal oxide substrates. By careful evaluation of changes in the C 1s binding energy between the spectra of thick and ultrathin polymer depositions, specific binding states of the polymer at the interface were observed. This allowed to identify the formation of a carboxylate ionic bond and hydrogen bonding at the solid/solid interface by XPS [12, 13].

Characterization of the thin acrylic polymer films by ambient pressure X-ray photoelectron spectroscopy (APXPS) and attenuated total reflectance Fourier transform infrared spectroscopy (ATR-FTIR) in the Kretschmann geometry allowed to characterize the chemical behavior of carboxylic functional groups with the aluminum (hydr)oxide surface in the presence of water. ATR-FTIR in the Kretschmann geometry allowed to identify the formation of a carboxylate bond *in situ* during the adsorption process of polyacrylic acid (PAA) and poly methyl methacrylate (PMMA) films respectively from a dilute polymer solution. Moreover, both techniques showed that water initially plays a beneficial role in the formation of this type of ionic bond, when the polymer/metal oxide system was exposed to an aqueous electrolyte [7, 8].

It has been shown that electrochemical reactions play an important role in the explanation of coating delamination. Scanning Kelvin Probe (SKP) allows to follow the onset of a delamination front *in situ* from a well-defined defect by monitoring the Volta potential [14]. This led to the proposal of a delamination mechanism for basic polymer coatings on steel by Leng and Stratmann [15-17]. The model was later extended to coated zinc substrates [18]. It was shown that the oxygen reduction reaction (ORR) plays a detrimental role in corrosive de-adhesion processes. SKP provides direct information of the corrosion potential under the coating, but it does not provide quantitative information on interfacial reaction rates. Therefore, Vijayshankar et al. used a hydrogen permeation based potentiometric approach to quantitatively determine the interfacial reaction kinetics of the oxygen reduction [19]. A Devanathan-Stachurski permeation technique, where hydrogen can permeate from one side of an iron-on-palladium membrane, is used to quantify the ORR rate at a buried polymer/metal oxide interface on the other side. However, the question is posed on how the electrochemical reactivity of such metal/polymer coated systems is determined by the interfacial chemistry of the metal oxide/coating interface. The aim of this work is to investigate the direct influence of chemical bonds at the interface on the overall delamination behavior.

Impedance spectroscopy is a versatile tool to monitor the water uptake kinetics and allows the quantification of the diffusion coefficient of water through the polymer [20, 21]. Additionally, water has a characteristic infrared signature, which is easily recognized in an infrared spectrum, leading to additional information on the diffusion rate [22-24]. Adhesive and corrosion properties of the polymer/metal oxide interface can be determined by EIS, but additional information on reactions at the interface is required for a good understanding of the occurring phenomena [25-27]. Therefore, a combination of both techniques into an integrated spectro-electrochemical technique provides multiple advantages when investigating electrolyte exposure on polymer/metal oxide systems. Vlasak et al. [28] reported studies of water diffusion through thin polymer coatings, recorded with an integrated spectro-electrochemical system combining conventional ATR-FTIR and impedance spectroscopy.

Where these studies focus on bulk phenomena such as water diffusion, it is our aim to study the effect of water molecules on the polymer/metal oxide interface. Öhman et al. introduced IR in the Kretschmann geometry to investigate the interfacial behavior of water at the solid/solid interface, combining this approach with conventional impedance spectroscopy [29-31]. In previous work, Pletincx et al. introduced an integrated spectro-electrochemical setup based on IR in the Kretschmann geometry and odd random phase multisine electrochemical impedance spectroscopy (ORP EIS) to monitor the effect of methanol adsorption onto an aluminum oxide surface [32]. By utilizing a metal coated internal reflecting element (IRE) in contact with a methanol solution, the evanescent field of the infrared light is able to reach the solvent/metal oxide interface and obtain an infrared spectrum resulting in information that is obtained directly from the interface region [30, 31, 33]. Impedance spectroscopy showed the chemisorption of methanol onto the aluminum oxide surface *in situ* and an electric equivalent circuit (EEC) model describing the adsorption behavior was proposed and proven statistically valid. The fitted parameters were linked to the infrared spectra, which allowed to explain the EEC in a physically meaningful manner.

This integrated approach is an ideal way to characterize the effect of an aqueous electrolyte on the polymer/metal oxide system and to study the stability of interfacial interactions *in situ* for long electrolyte exposure times. Moreover, the integrated setup is not restricted to ultrathin model polymers as used in this work. The setup is suited for any type of polymer deposition, ranging from model polymer films to thick layers of complex industrial coating formulations.

In this work, the effect of an aqueous electrolyte on the interface of an ultrathin polyacrylic acid (PAA)/aluminum oxide system is studied as a function of time using the integrated spectro-electrochemical setup. ATR-FTIR in the Kretschmann geometry provides an interface-sensitive and *in situ* analysis of a polymer/metal oxide interface. By utilizing a random phase multisine excitation signal for the ORP EIS analysis, a shorter measurement time is achieved since all frequencies are excited simultaneously. Therefore, the ORP EIS measurement time is in an equal time-frame as the one for obtaining an infrared spectra. A comparison of the trends observed by both techniques in the integrated setup is therefore allowed.

ORP EIS results in the characterization of electrochemical properties of the whole polymer/metal oxide system. The impedance, the magnitude of the measurement noise, the level of the nonlinear response and the level of nonstationary behavior of the system are measured at each frequency for a given excitation amplitude and can be quantified by ORP EIS [34]. Additionally, validation of the fitting quality of the proposed equivalent circuit is possible by comparing the experimental noise levels with the complex residuals of the fitted model [35-37].

Afterwards, the results obtained for the polymer/*PVD aluminum oxide* system are compared with similar measurements on different types of aluminum oxide sheets. The first type is a native oxide for which the metal substrate was etched in an alkaline solution and then exposed to ambient conditions to form a *native aluminum oxide*. This oxide type has similar thickness but a different metallurgy than the PVD deposited oxide system [38]. The second oxide type is an *anodized aluminum oxide* substrate, of which the oxide is a carefully controlled barrier oxide. XPS is utilized to characterize the surface of all three oxide types and to link the oxide surface's acid-base properties with the observations of the (spectro-)electrochemical setup.

Finally, a comparison is made with a PMMA deposition. PAA has a polymer chain with a carboxylic acid functional group whereas PMMA contains a methyl methacrylate repeating unit. Therefore, both polymers have a different adsorption mechanism onto the aluminum oxide surface as shown in previous work [7]. Therefore, by making a comparison between these two polymer types, the polymer/metal oxide interfacial stability under electrolyte exposure is investigated.

2. Materials and methods

2.1. Model oxide preparation

For the ATR-FTIR in the Kretschmann geometry, a germanium internal reflection element (IRE) crystal was coated with pure aluminum (99.99% metals basis, Johnson Matthey) by means of a high-vacuum evaporation coating system (VCM 600 Standard Vacuum Thermal Evaporator, Norm Electronics). The thickness of the physically vapour deposited (PVD) aluminum film is 50 nm, as determined with a quartz crystal microbalance (QCM). The PVD deposited aluminum surface was exposed to the ambient environment to form a passive oxide layer. This oxide system is denoted as *PVD aluminum oxide* in the manuscript. Within 10 min after metal deposition, the surface was exposed to the polymer solution.

To compare the observations of the integrated spectro-electrochemical setup and to evaluate the effect of the oxide type's influence on the interfacial interactions, similar ORP EIS measurements are conducted on two types of rolled aluminum oxide substrates. Here, the metal substrates were cut from a 0.3 mm ultrapure aluminum sheet (99.99% metals basis, rolled sheet, Norsk Hydro Aluminium). Samples were rinsed ultrasonically in acetone for 5 min. After cleaning, the samples were chemically etched in a 25 g L^{-1} NaOH solution (Pellets, VWR Chemicals) for 1 min. Then the samples were rinsed with H_2O and blown dry with nitrogen and exposed to atmosphere to let natural oxide growth occur. This oxide system is denoted as *native aluminum oxide* in the manuscript.

Anodized samples were prepared from the same 0.3 mm ultrapure aluminum sheet (99.99% metals basis, rolled sheet, Norsk Hydro Aluminium). The samples were ultrasonically cleaned in acetone and etched in a 25 g L^{-1} NaOH solution for 1 min. After rinsing and drying, the samples were galvanostatically anodized with a current density of 5 mA/cm^2 in a 3% diammonium tartrate (VWR Chemicals) solution at 25 °C, with the voltage going up to 20 V. This corresponds with the formation of a barrier-type oxide with a thickness of approximately 20 to 30 nm. This oxide system is referred to as *anodized aluminum oxide*.

2.2. Polymer deposition by reactive adsorption

Thin polymer films of poly acrylic acid (PAA) were deposited by reactive adsorption on the different aluminum oxide substrates from a 0.1% w/w PAA (Sigma Aldrich, Mw = 450,000 g mol^{-1}) solution in methanol (99.8% ACS, VWR Chemicals). For the PMMA deposition, this was done from a 0.1% w/w PMMA (Sigma Aldrich, Mw = 250,000 g mol^{-1}) solution in toluene (99.5% ACS, VWR Chemicals). After 24 h, the samples were removed from the solution. Next, the substrates were immersed in pure solvent to remove remaining physisorbed molecules from the oxide surface.

2.3. Analysis methods

2.3.1. Spectro-electrochemical setup of odd random phase EIS and ATR-FTIR in Kretschmann geometry

A Thermo-Nicolet Nexus Fourier transform infrared device with a mercury-cadmium-telluride (MCT) liquid-nitrogen-cooled detector, and a nitrogen-purged VeeMAX III ATR measurement accessory are used. The resolution of the acquired spectra is set to 4 cm^{-1}. OMNIC 8.1 software package (ThermoElectron Corporation, Madison, WI) was used to control the spectrum acquisition. On top of the polymer coated native oxide film, the electrolyte is placed in a electrochemical cell from PIKE Technologies to measure the effect of the aqueous solution *in situ* at the interface. A spectrum of the germanium crystal coated with aluminum oxide and the polymer deposition is used as a background spectrum. By using this background spectrum, changes at the interface are observed in the spectra after electrolyte exposure.

The thickness of the deposited metal film and the utilized angle control the probing depth of the evanescent wave. Here, a PVD film thickness of about 50 nm (QCM determined) and a grazing angle are used. The evanescent wave of infrared light is largely absorbed by the PVD deposited film, therefore this field is just able to reach the interface region, leading to a probing depth of the order of nanometers and results in a near-interface spectrum. A more detailed description of this technique is given by Öhman et al. [30].

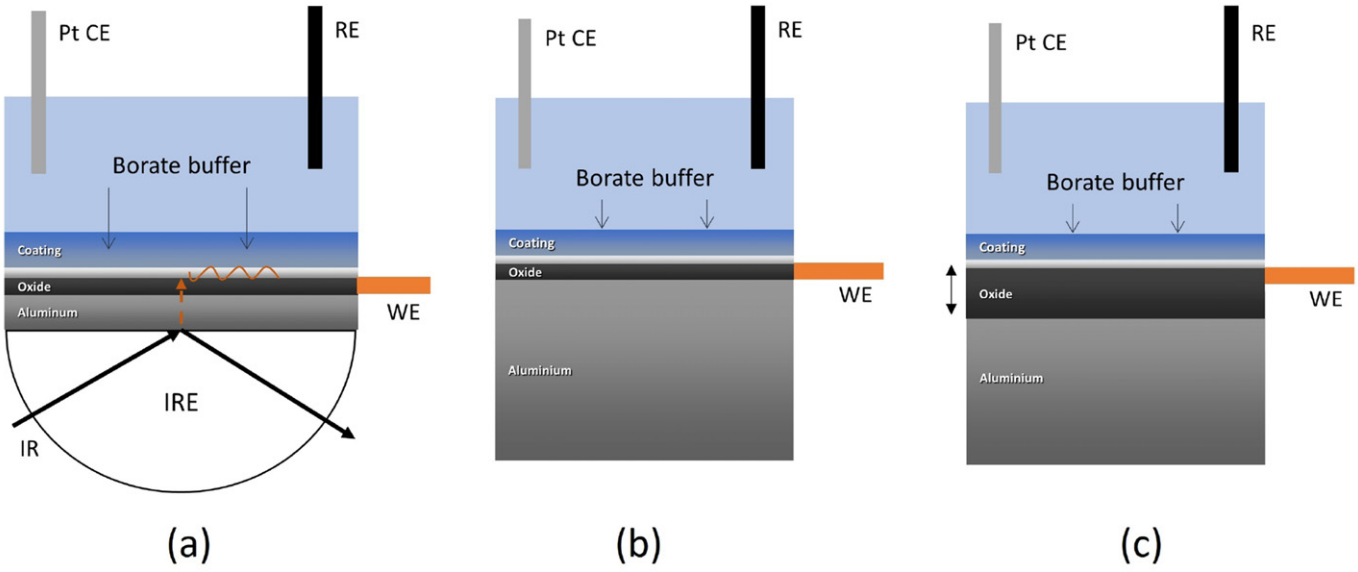

Fig. 1. Schematic representation of (a) the integrated spectro-electrochemical setup with the polymer coated onto the *PVD aluminum oxide* film, (b) ORP EIS setup of the polymer coated/*native aluminum oxide* and (c) ORP EIS setup of the polymer coated on *anodized aluminum oxide*. The polymer/metal oxide systems are exposed to a 0.1 M borate buffer solution.

Simultaneously, impedance spectra were recorded by using a three-electrode setup. A Biologic SP-200 potentiostat and a National Instruments PCI-4461 data acquisition(DAQ-)card are utilized. A platinum wire is used as counter electrode and a Ag/AgCl electrode as reference. Copper wire is attached to the PVD deposited aluminum oxide to create the working electrode and special care was taken not to bring the Cu-wire in contact with the aqueous solution. The electrolyte used in the electrochemical cell is a 0.1 M borate buffer (prepared by a mixture of sodium tetraborate and boric acid (VWR Chemicals)) to investigate the effect of water at the interface. Paraffin film was used to wrap around the counter- and reference electrode in order to seal the electrochemical cell and to minimize evaporation of the electrolyte. The odd random phase multisine perturbation consists of the sum of harmonically related sine waves with equal amplitude and random phases. The applied signal is a 10 mV RMS variation around the open circuit potential. Groups of 3 consecutive odd harmonics are excited of which one harmonic is randomly omitted. At all measured excited and non-excited frequencies, both the potential and the current signals are measured. The technique is described in detail elsewhere [35, 39, 40]. The multisine signal was generated with MATLAB R2013a software (MathWorks Inc.). Control of the DAQ-card and processing of the collected data was also

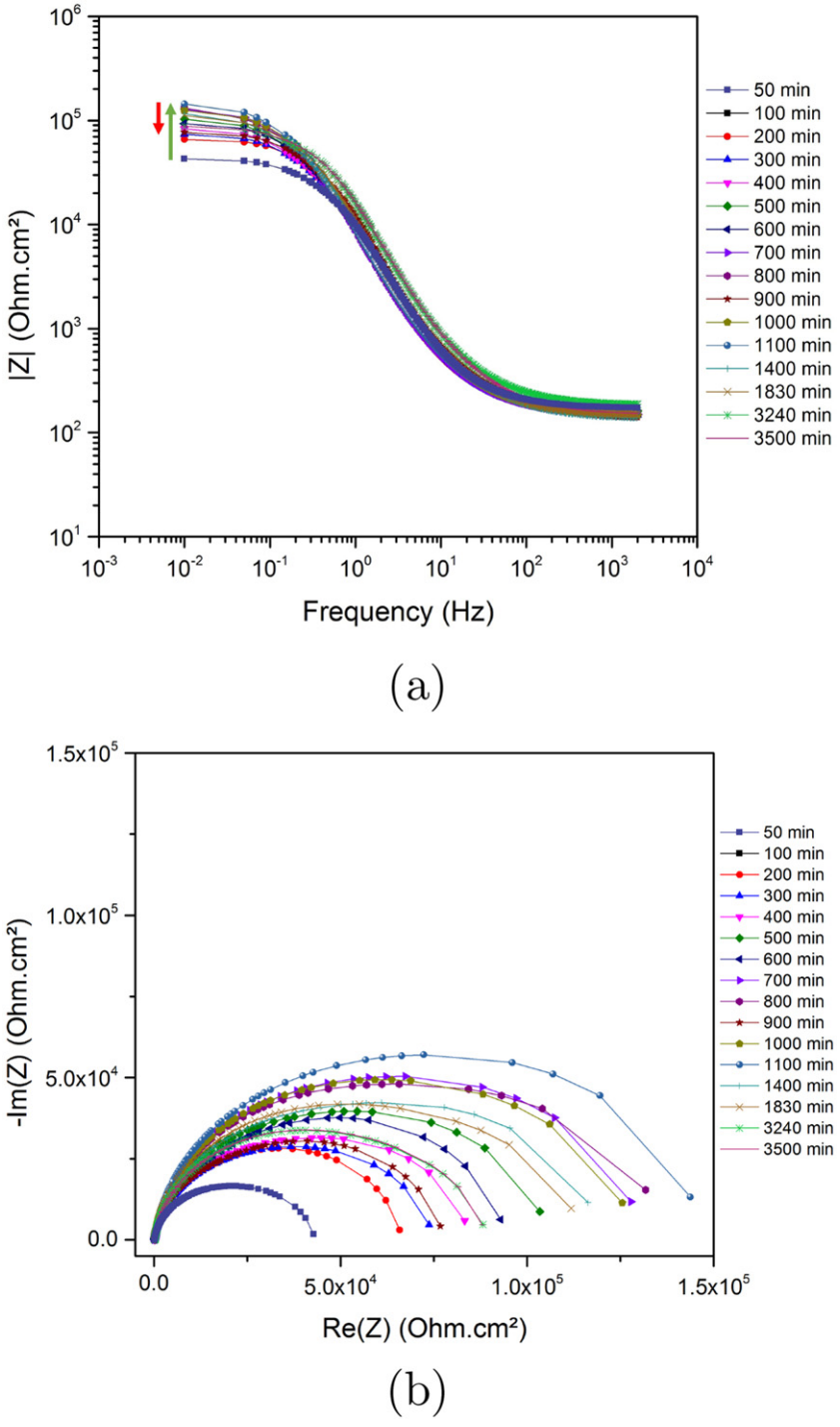

Fig. 2. (a) Magnitude Bode plot and (b) Nyquist plot of the *PVD aluminum oxide* coated with PAA as a function of exposure time to the 0.1 M borate buffer electrolyte.

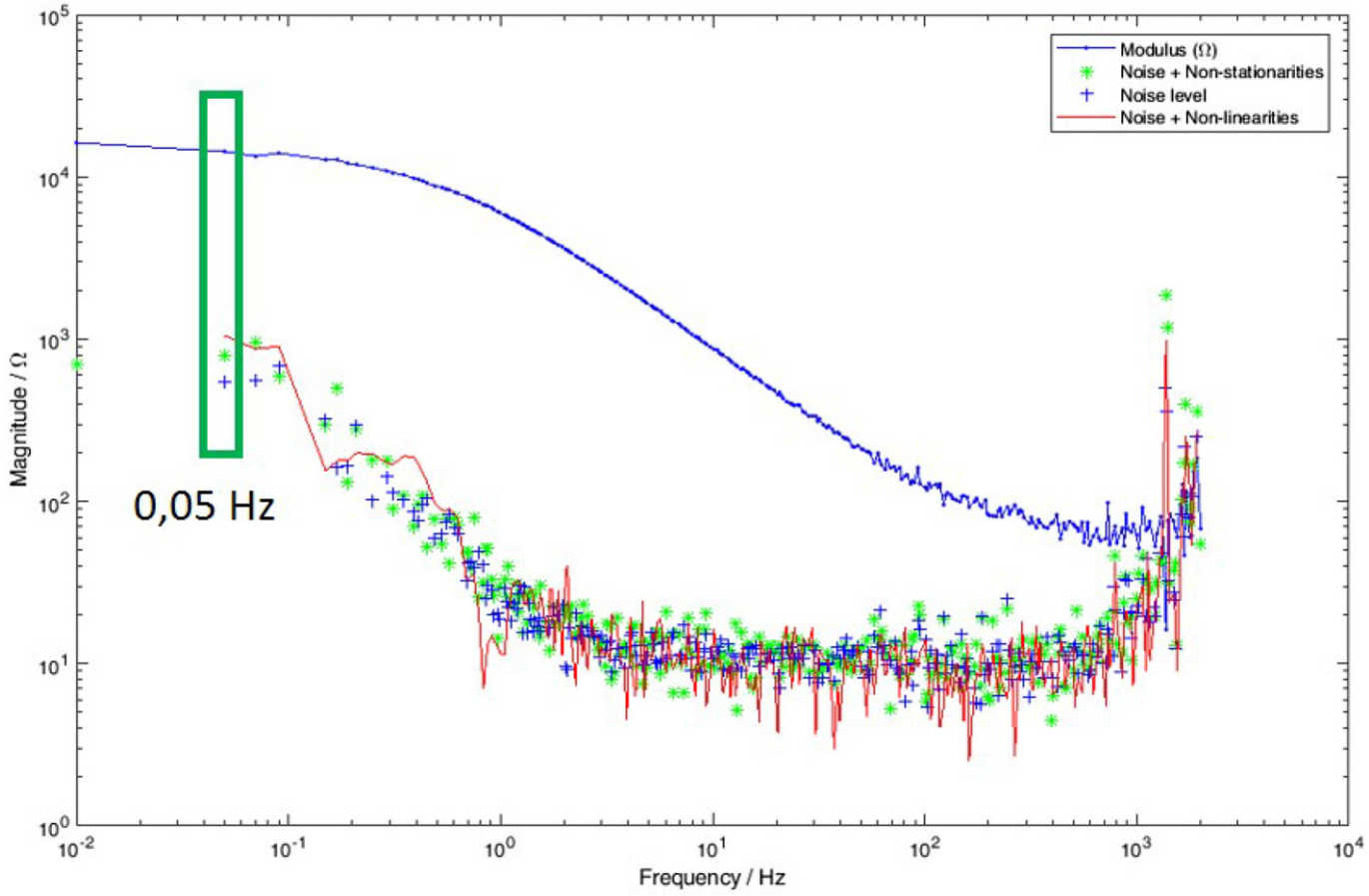

Fig. 3. Bode plot of the impedance magnitude containing the experimental data, noise curve, noise on the excited frequencies and noise on the non-excited frequencies of the measurement after 1 h borate buffer exposure. The system behaves linear and stationary at all frequencies since all noise levels are overlapping. The impedance magnitude and related noise levels in the low frequency region (0.05 Hz) are selected to compare with the infrared data.

achieved with MATLAB software. Impedance spectra are recorded every 600 s between 0.01 and 2000 Hz.

ORP EIS measurements for the native and anodized aluminum oxide metal sheets were conducted with the same three-electrode setup Biologic SP-200 potentiostat and a National Instruments PCI-4461 data acquisition(DAQ-)card. Equal excitation parameters and 0.1 M borate buffer were used. Impedance spectra are recorded every 600 s between 0.01 and 10^4 Hz. In Fig. 1, a schematic representation is shown of the integrated setup and the setup for the two different aluminum oxide types.

2.4. X-ray photoelectron spectroscopy

X-ray photoelectron spectroscopy (XPS) measurements were conducted with a PHI-5000 Versaprobe II (Physical Electronics) utilizing a Al Kα monochromatic X-ray source (1486.71 eV photon energy) with a spot diameter of 100 µm to measure surface compositions up to ca. 10 nm in depth. The irradiation power of the X-ray beam was 25 W. The kinetic energy of the photoelectrons was measured with a take-off angle of 45°. The vacuum in the analysis chamber was better than 1×10^{-9} Torr. Dual beam charge neutralization was utilized to compensate potential charging effects. A pass energy of 187.85 eV and an energy step size of 0.1 eV are used to record survey scans. PHI Multipak software (V9.5) is used to analyze the obtained XPS data. High resolution scans of the O 1s peak are obtained with a pass energy of 23.5 eV and 0.05 eV energy step size. For the fitting procedure of the O 1s peak, the software CasaXPS was used. The peak shape is a mixed Gaussian-Lorentzian, with a Shirley type background.

2.5. Secondary electron microscopy

For secondary electron microscopy (SEM) imaging, a JEOL JSM-IT300 equipped with a tungsten filament source is utilized. An acceleration voltage of 10 kV was used together with a working distance of 10 mm.

3. Results and discussion

3.1. Spectro-electrochemical analysis of PAA deposited on PVD aluminum oxide exposed to borate buffer

3.1.1. Odd random phase multisine electrochemical impedance spectroscopy

The Bode plot (left) and the Nyquist plot (right) of the *PVD aluminum oxide* coated with PAA during different exposure times to the borate buffer are shown in Fig. 2. An evolution in the low frequency range of the magnitude of the impedance modulus is observed. More specifically, an increase in the magnitude of the modulus is observed during the first 1000 min, afterwards, a decrease in the magnitude is observed. The Nyquist plot show part of a semi-circle that follows the same trend, increasing during the first 1000 min after which its size decreases again.

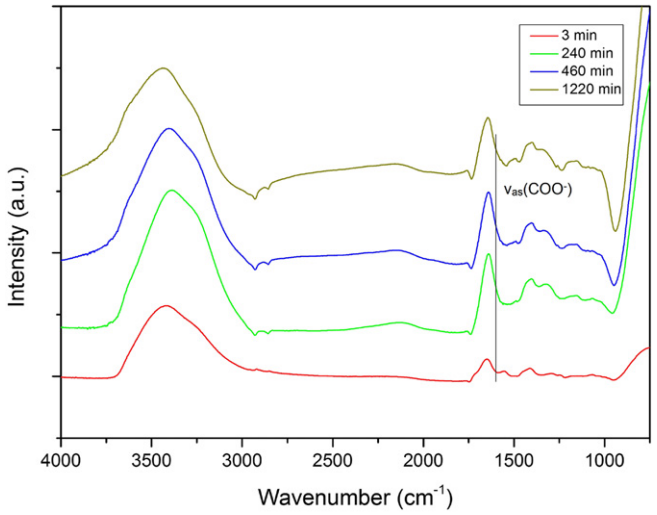

Fig. 4. Infrared spectra selected at various borate buffer exposure times. The asymmetric carboxylate at 1610 cm^{-1} is specific for the ionic bond at the polymer/metal oxide interface and is selected to be monitored as a function of exposure time.

Since ORP multisine EIS is utilized, an evaluation of the stationarity and linearity at the given excitation signal of 10 mV is made possible [35-37, 41]. The magnitude and phase Bode plots after one hour of borate buffer exposure are shown in Fig. 3 together with the noise curve, the *noise + non-linearities* curve and the *noise + non-stationarities* curve. Since the curve of the *noise + non-linearities* overlaps with the noise level, the system behaves linear. It is also concluded that the system behaves stationary as the *noise + non-stationarities* curve overlaps with the experimental noise curve. One example is shown in Fig. 3, but this overlap of noise levels is valid for every recorded measurement cycle. It is observed that these curves make a nearly exact overlay with the experimental noise and it is thus valid to use an electric equivalent circuit in order to model the obtained impedance measurements.

3.1.2. Infrared spectroscopy in the Kretschmann geometry

The evolution of the spectra at the interface between the *PVD aluminum oxide* layer coated with the ultrathin PAA layer is shown in Fig. 4 for selected exposure times of the polymer/metal oxide system to the borate buffer. Since the background spectrum is the *PVD aluminum oxide* after polymer deposition in contact with ambient air, all the changes at the interface are observed in the obtained spectra. Positive peaks show molecular vibrations of functional groups that build up or are formed at the interface and negative peaks indicate functional groups that are disappearing from the interface with respect to the initial (not exposed to the electrolyte) state of the polymer/metal oxide.

Immediately after exposure to the borate buffer, peaks indicating water build-up at the interface are observed. These peaks are located around 3500 and 1650 cm^{-1}. The bands between 3000 and 2800 cm^{-1} are assigned to CH_2 stretching. These peaks are negative, indicating the replacement of CH_2 groups from the polymer backbone at the interface by the water molecules. Positive bands in the region of 1450–1620 cm^{-1} indicate that carboxylate species are formed at the interface after electrolyte exposure. The peak at 1610 cm^{-1} is assigned to the $\nu_{as}(COO^-)$ carboxylate stretch, highlighted in Fig. 4. The symmetric carboxylate stretch $\nu_s(COO^-)$ can be found at 1442 cm^{-1} and 1502 cm^{-1}. The continuously decreasing negative peak at 952 cm^{-1} is assigned to the ν(Al—O) of free surface hydroxyl groups on aluminum oxide, showing the consumption of this functional group at the interface. This trend reveals that the surface hydroxyl groups interact in the ionic bond formation at the interface. A more detailed peak assignment of this system and the proposed adsorption mechanism of PAA on aluminum oxide is discussed in previous work [8].

The advantage of the integrated spectro-electrochemical setup is that information is obtained *in situ*. Moreover, the impedance data is recorded in the same time-frame as the FTIR data, since a multisine signal is applied. This allows to make a direct comparison of observations obtained with both techniques. From the infrared spectra, the peak intensity of the $\nu_{as}(COO^-)$ carboxylate stretch located at 1610 cm^{-1} is selected after baseline correction and is plotted as a function of exposure time (peak location shown in Fig. 4). From the ORP EIS Bode plot, changes at the low frequency range are observed. Therefore, the magnitude and error value of the impedance value

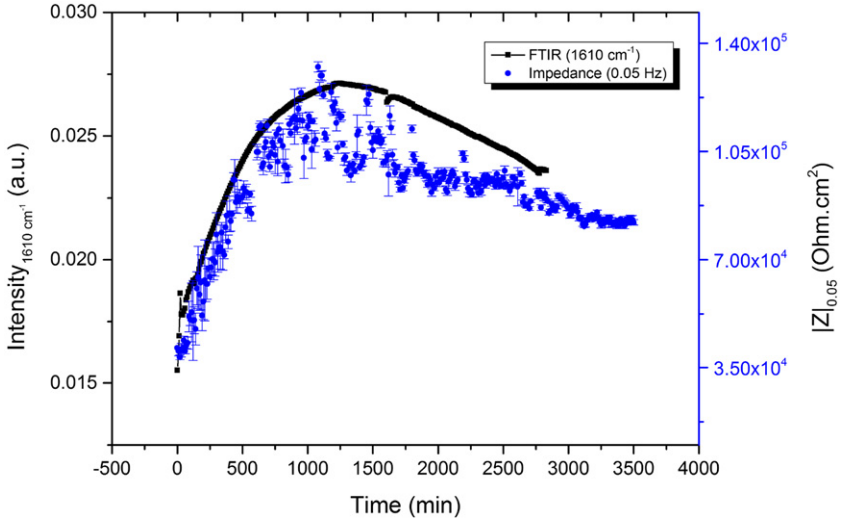

Fig. 5. Overlay of FTIR and Impedance data. The intensity of the asymmetric $\nu_{as}(COO^-)$ carboxylate stretch located at 1610 cm^{-1} and baseline corrected as a function of electrolyte exposure time (black dotted line) obtained with FTIR in the Kretschmann geometry; Magnitude and error values of the impedance at 0.05 Hz (blue dots). A direct link is observed between the carboxylate bond at the interface and the impedance magnitude from the low frequency region.

at 0.05 Hz is selected (shown in Fig. 3). In Fig. 5, these two selected parameters are plotted as a function of electrolyte exposure time. A direct link is observed between the carboxylate stretch, indicative for the ionic bond at the interface and the trend of the magnitude values of the impedance in the low frequency range. During approximately the first 1000 min, an increase in the FTIR peak intensity indicates that more ionic bonds are being formed at the interface. This corresponds with an increase of the magnitude of the impedance, because the bond formation increases the resistance for the electric current transfer. After these 1000 min, the IR intensity of the carboxylate stretch decreases as well as the impedance magnitude. This corresponds with a replacement of the ionic bonds at the interface due to water build-up and macroscopically leads to a delamination of the organic coating. Since there is a larger exposed metal oxide surface, this leads to a lower resistance value.

This macroscopic delamination is observed when comparing the SEM micrographs of a PAA coated aluminum oxide before and after borate buffer exposure, shown in Fig. 6. In Fig. 6a, the pristine PAA coated aluminum oxide surface is observed without any inhomogeneity. The polymer layer is sufficiently thin. Hereby, the surface structure of the etched aluminum oxide is observed through the polymer deposition. When comparing this with Fig. 6b, clear cracks and delaminated zones are observed. It can thus be concluded that the exposure of the hybrid system to the aqueous electrolyte leads to a destruction of the ionic bonds at the interface as a result of water diffusion and macroscopically leads to delamination. In Fig. 6b, it is observed that no corrosion products have formed during electrolyte exposure. Since a borate buffer is used in the pH range of 8, a passive aluminum oxide surface is formed. The use of a buffer keeps the pH stable in the passivation region of the aluminum, preventing the metal to dissolve. This allows us to only monitor interfacial changes induced by the diffusion of the electrolyte and excluding any corrosion-induced delamination phenomena.

3.2. Proposed electrical equivalent circuit (EEC) to describe the PAA/aluminum oxide system exposed to an aqueous electrolyte

From the ORP multisine EIS analysis, it was shown that the system behaves both linear and stationary. Therefore, it is allowed to propose an EEC to model the impedance data. In Fig. 7a, the circuit is shown. Here, R_{Elec} represents the electrolyte resistance. R_1 and Q_1 are the resistance and constant phase element representing the PAA film. R_2 and Q_2 are the resistance and constant phase element are assigned to the aluminum oxide layer response. No other contributions are expected to describe the polymer/metal oxide system, indicating the physical validity of the proposed model.

The quality of the used model can be evaluated from Fig. 8, where the proposed EEC (Fig. 7a) is fitted onto the experimental data. A Levenberg-Marquardt method is used to vary the electrochemical parameters in order to minimize the distance between the impedance-frequency equations of the model and the obtained impedance values. Additionally, the data is weighted by the noise values. This results in fitted electrochemical parameters and their standard deviation. The ORP EIS approach also allows to compute the complex residual of the fitted data. By comparing this complex residual with the experimental noise data, a goodness of fit can be determined. A nearly perfect overlap between the complex residual and the experimental noise is observed, which is a condition for the validity of the model. This is the second condition that is met for accepting the model, next to the physical relevance of the proposed model. The complex residual stays near the noise levels (with all values under 10%) for every measurement cycle, therefore the goodness of fit is accepted for all measurements over the entire exposure time. Since the raw impedance values are extracted directly from the potentiostat without any compensation procedure, the noise levels increase above a frequency of 10^3 Hz. This compensation procedure

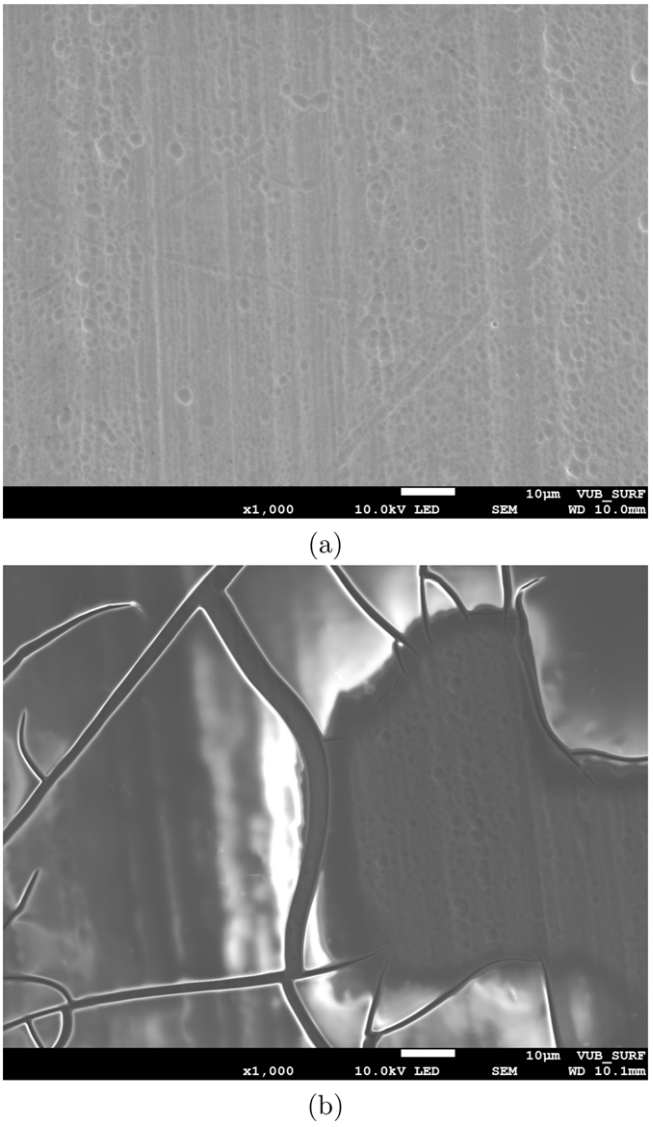

Fig. 6. SEM micrographs of a PAA coated aluminum oxide substrate (a) before borate buffer exposure and (b) after 3 days of borate buffer exposure. The aluminum oxide substrate is an alkaline etched native oxide.

is typically built-in by the manufacturer in the operating software of the potentiostat, but is absent in the custom built ORP EIS software. This leads to a low signal-to-noise ratio from this frequency on but in the high frequency region only the influence of the electrolyte resistance is present. Fortunately, the electrolyte resistance is easily modelled from the ORP EIS data, despite this relatively high signal-to-noise ratio. The value of the electrolyte resistance varies around 150 Ohm·cm^2, which is a reasonable value for the electrolyte resistance. The fitted values of the constant phase element (CPE) of the organic film (Q_1) has a value that varies around 30 ± 4.5 µF/cm^2. The thickness of polymer film can be estimated from this value, assuming the dielectric constant (ϵ) of the polymer layer is 1.6 (value for polyethylene). This gives an estimated thickness of 4.7 ± 0.3 nm. This estimation corresponds well with previous work [8, 42]. When looking at the fitted values of the constant phase element (CPE) of the oxide layer (Q_2), a value around 100 ± 2.2 µF/cm^2 is obtained. If an assumption of the dielectric constant (ϵ) for aluminum oxide is taken to be 9.1, then a thickness estimation of 2.9 ± 0.1 nm is retrieved. This value corresponds well with the average thickness of passive aluminum oxide layers [43].

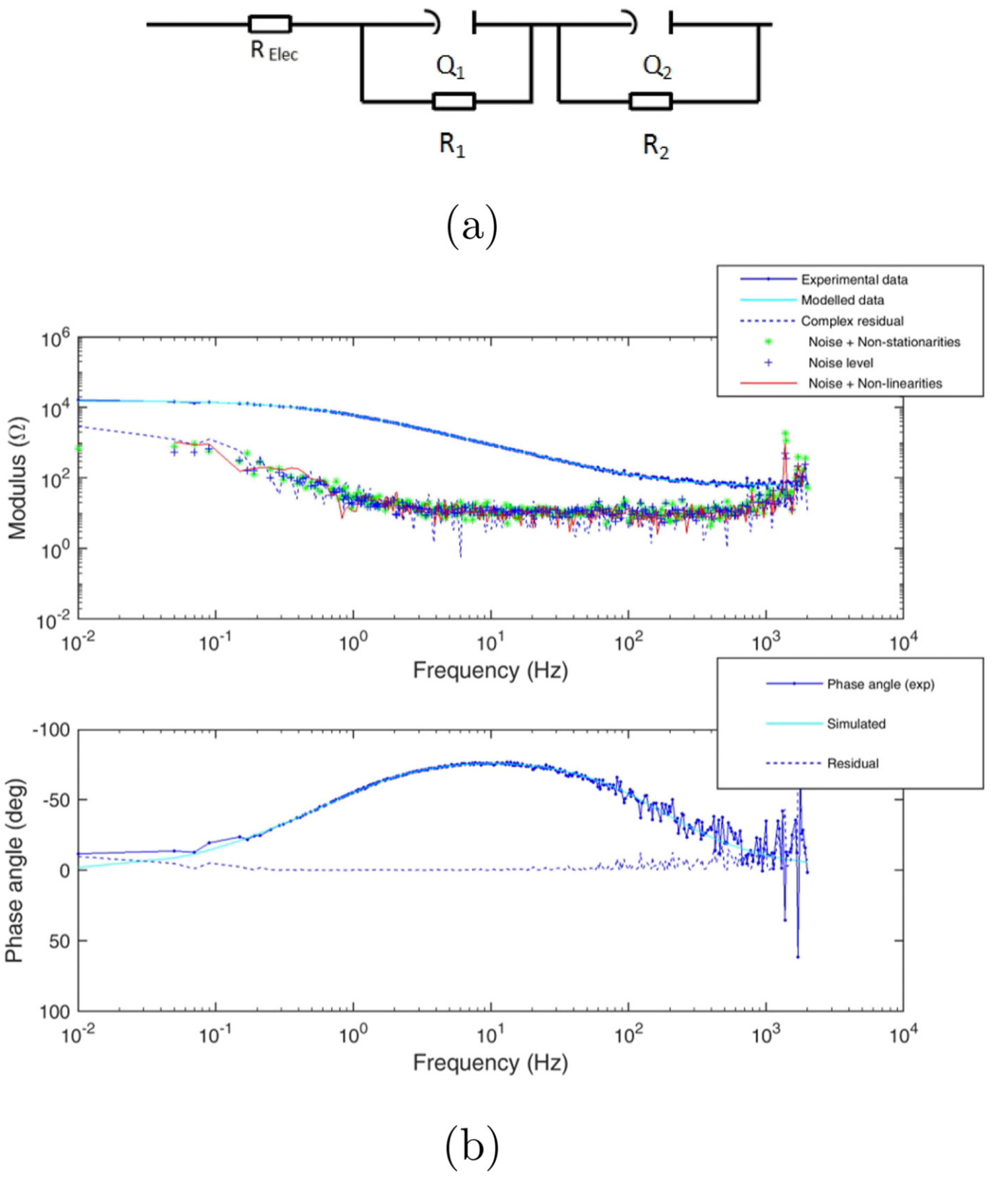

Fig. 7. (a) Equivalent electrical circuit to describe the PAA coating on aluminum oxide. The first time constant describes the organic layer (resistance R_1 and constant phase element Q_1), the second time constant describes the aluminum oxide layer response (resistance R_2 and constant phase element Q_2). (b) Bode magnitude and phase plot containing the experimental data, modelled curve, complex residual, noise levels, noise on the excited frequencies and noise on the non-excited frequencies of the measurement at 1 h of exposure to the electrolyte.

In Fig. 8, the fitted resistance values with the EEC (Fig. 7a) are shown. Resistance values of the organic coating (R_1) and resistance values of the interface and oxide layer (R_2) as a function of electrolyte exposure time are plotted. An increasing trend of the resistance of R_1 is observed till approximately 1000 min, after which the resistance reaches a plateau level. This can be explained because of the response of the carboxyl groups of PAA. Due to the diffusion of the borate buffer, the carboxylic acid functional groups of the polymer deprotonate. This deprotonation leads to an acidification of the electrolyte in the organic layer. Since a borate buffer is used to maintain a constant pH, the borate buffer compensates this acidification. As the buffer is a mixture of a weak acid and its conjugated base, the acidification is compensated by shifting the equilibrium of the not-completely ionized acid. This leads to a decrease of ion concentration in the electrolyte and results in an increase in resistance of the organic layer (R_1). This continuous up till the point that all the functional groups are deprotonated by the diffusing electrolyte, and this explains the plateau reached by the resistance values. For the resistance (R_2) assigned to the interface and oxide layer, the same trend is followed as the impedance values in the low frequency range. The same interpretation for the trend of the resistance values can be given as discussed earlier, where the trend of the IR values of the carboxylate stretch follows a similar trend. Indicating that the changes at the polymer/metal oxide interface lead to the variations in the

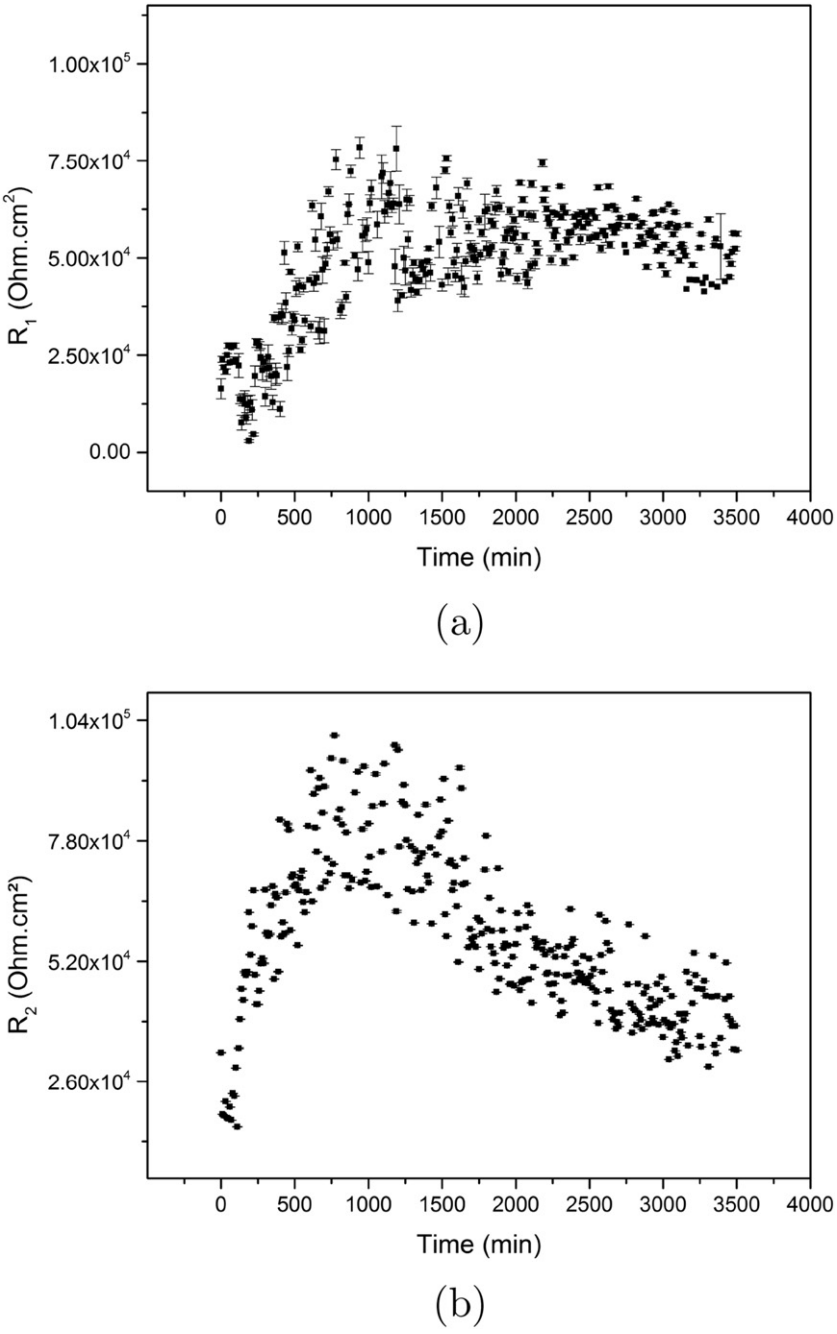

Fig. 8. Fitted resistance values with the EEC shown in Fig. 7a. Resistance values of the organic coating (R_1) and resistance values of the interface and oxide layer (R_2) as a function of electrolyte exposure time.

resistance values. This allows us to assign the changes of resistance R_2 to the changes occurring at the polymer/metal oxide interface. A third and final condition to validate the proposed model is that all parameters have reasonable values. Given the discussion, it is concluded that all three conditions for validity are met and that the proposed model is conclusive to describe borate buffer exposure to the PAA/aluminum oxide system.

3.3. Comparison with different oxide types

To elucidate the effect of the aluminum oxide type on the stability of the polymer/metal oxide interface, the type of oxide is varied in the ORP EIS measurements. Samples are still coated with 0.1 wt % PAA in methanol to form an ultrathin film. The first oxide type is etched in 25 g L^{-1} NaOH to remove the oxide and is afterwards rinsed with H_2O and exposed to the ambient environment to create a passive oxide layer (*native aluminum oxide*). This oxide type has a similar thickness as the oxide formed on the PVD deposited aluminum substrate, but a different metallurgy exists between these two types. The second oxide type is an *anodized aluminum oxide* with a thicker barrier oxide layer. In Fig. 9, the Bode and Nyquist plots of the *native aluminum oxide* coated with PAA and the *anodized aluminum oxide* coated with PAA are shown as a function of electrolyte exposure time. For the *native aluminum oxide*, a similar trend is noted as for the *PVD aluminum oxide*. An evolution in the low frequency range of the magnitude of the impedance modulus is observed. More specifically an increase in the magnitude of the modulus is observed during the first 1000 min, afterwards a decrease in the magnitude is recognized similar to the observations for the PVD deposited type. The Nyquist plot shows a similar trend. For the *anodized aluminum oxide*, the Bode

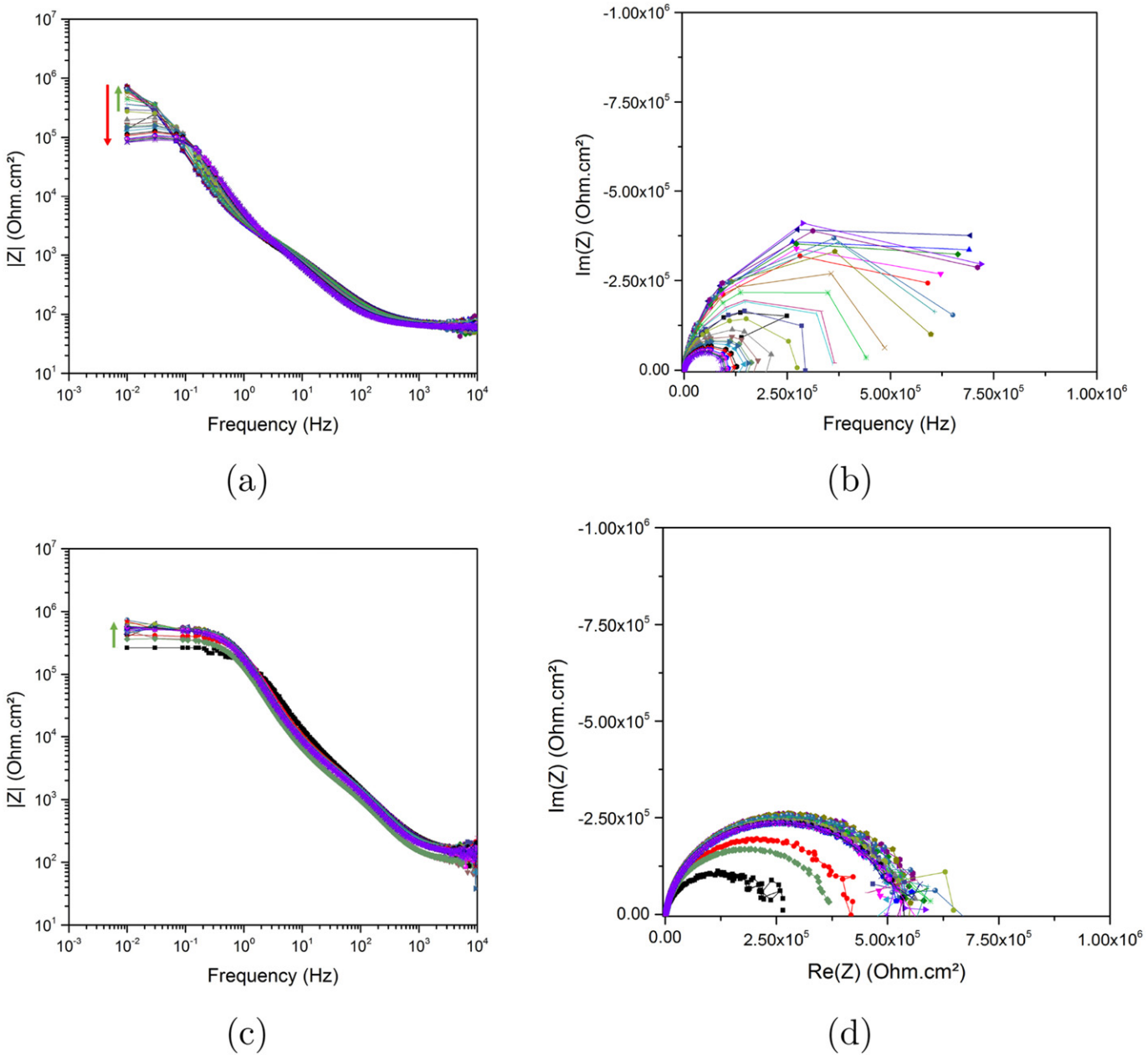

Fig. 9. Bode plot and Nyquist plot of the *native aluminum oxide* coated with PAA ((a)–(b)) and *anodized aluminum oxide* coated with PAA ((c)–(d)) as a function of exposure time to the 0.1 M borate buffer electrolyte.

plot marks an increasing trend in the low frequency range, but then stays constant. Also, the semi-circle in the Nyquist plot follows this trend.

In Fig. 10, the Bode plot of the impedance magnitude containing the experimental data, noise curve, noise on the excited frequencies and noise on the non-excited frequencies of the measurement after 1 h borate buffer exposure for PAA coated *native aluminum oxide* and PAA coated *anodized aluminum oxide* substrates are shown. Both systems behave linear and stationary at all frequencies since all noise levels are overlapping. The impedance magnitude and related noise levels in the low frequency region (0.05 Hz) are selected to compare with PAA coated *PVD aluminum oxide*, their respective trends are shown in Fig. 11.

Here, it is observed that the impedance magnitudes of PAA coated *native aluminum oxide* follow a similar trend as those of PAA coated *PVD aluminum oxide*. An initial increase in ionic bond/impedance value is followed by a decrease indicating a delamination of the polymer layer. For the *anodized aluminum oxide*, an initial trend is observed in the impedance values in the low frequency range and this increase is not followed by a delamination step of the polymer/metal oxide system. This indicates that the *anodized aluminum oxide* leads to a more stable interface. In order to unravel this observation, XPS analysis of the surfaces of the non-coated aluminum oxide types is conducted.

In Fig. 12, the O 1s spectra of blank *PVD*, *native* and *anodized* aluminum oxide are presented [44, 45]. The spectra are fit with contributions for the metal oxide (O^{2-} peak) at a binding energy of 530.4 eV. For the hydroxyl groups, an OH peak is added at 1.2 eV (w.r.t. O^{2-} peak) and an adsorbed H_2O peak is added to the model at 2.4 eV (w.r.t. O^{2-} peak). The fitted spectra of the PVD and native oxide demonstrate a similar contribution of the hydroxyl fraction. From literature, it is known that the OH fraction of the metal oxide surface is directly related to the amount of bonds formed at a polymer/metal oxide interface [44, 46-52]. In our FTIR spectra, the O—H peak located at 952 cm^{-1} decreases upon electrolyte exposure. This exposes that the free surface hydroxyl groups interact with the polymer to form interfacial bonds. The similar hydroxyl content observed in the O 1s spectra can explain the similar stability observed in the impedance data for the PVD deposited aluminum oxide (41% conc.) and the native aluminum oxide (49% conc.). The O 1s data of the anodized aluminum oxide evidence that this oxide type has a much larger hydroxyl contribution (61% conc.) than the other two oxide types. This can be linked to the observation of the impedance values of the low frequency range, where a stable region is observed for the given exposure time. This observation shows that more hydroxyl groups at the aluminum oxide interface lead to a more stable polymer/metal oxide interface as more ionic bonds were formed before exposure to the electrolyte. The ORP EIS methodology presented in this work allows to determine the behavior of the polymer/metal oxide interface. It is shown that the amount of free surface hydroxyl groups on the oxide surface have a large impact on the formation of chemical interactions at the polymer/metal oxide interface, as observed in previous investigations. These observations validate the followed methodology and the ORP EIS interpretation, proposed in this work.

3.4. Comparison with PMMA depositions on aluminum oxide

PAA has a polymer chain with a carboxylic acid functional group whereas PMMA contains a methyl methacrylate repeating unit. Therefore PMMA is selected to investigate the stability at the aluminum oxide interface by making a comparison between these two polymer types. In previous work, a set of surface analysis techniques was utilized to characterize the formed hydrogen and ionic bonds during reactive adsorption and to describe the effect of water on the interface. It was demonstrated that water plays a mediating role at the interface, where hydrolysis of the methoxy group leads to the formation of methanol and a carboxylic acid functional group that forms the ionic bond by interacting with the free surface hydroxyl groups of the aluminum oxide [7].

The Bode plot of the impedance magnitude containing the experimental data, noise curve, noise on the excited frequencies and noise on the non-excited frequencies of PMMA/aluminum oxide after 1 h borate buffer exposure are shown. The system behaves linear at all frequencies since the experimental noise level and the *noise and non-linearities* curve are overlapping. A small level of non-stationarity is

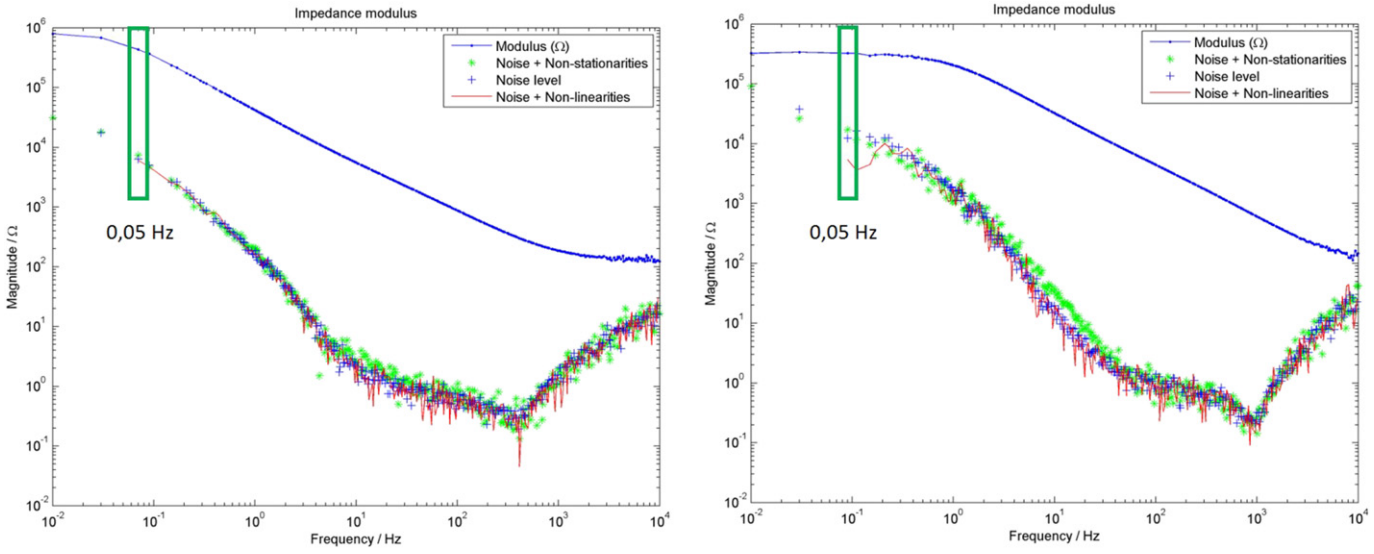

Fig. 10. Bode plot of the impedance magnitude containing the experimental data, noise curve, noise on the excited frequencies and noise on the non-excited frequencies of the measurement after 1 h borate buffer exposure for PAA coated *native aluminum oxide* (left) and PAA coated *anodized aluminum oxide* (right). The system behaves linear and stationary at all frequencies since all noise levels are overlapping. The impedance magnitude and related noise levels in the low frequency region (0.05 Hz) are selected to compare with PAA coated *PVD aluminum oxide*.

observed in the frequency range of 50 Hz–1 kHz, however, when monitoring the instantaneous impedance levels, this amount of non-stationarity can be neglected and modelling the data with an EEC is reasonable.

An identical EEC is used to describe the PMMA/aluminum oxide hybrid system as the one used for the PAA/aluminum oxide depositions (Fig. 7a). R_{Elec} represents the electrolyte resistance. R_1 and Q_1 are the resistance and constant phase element representing the PMMA film. R_2 and Q_2 are the resistance and constant phase element mimicking the polymer/metal oxide interface and the electrochemical behavior of the oxide layer. In Fig. 13, the fitting quality of the proposed model can be evaluated and a good overlap between the complex residual of the fitting and the experimental noise levels is observed. This indicates the goodness of fit of the proposed EEC and the electrochemical parameters and their standard deviations are obtained. The value of the electrolyte resistance varies around 150 Ohm·cm^2. The fitted values of the constant phase element (CPE) of the organic film (Q_1) and the oxide film (Q_2) are respectively in the range of 20 μF/cm^2 and 1 μF/cm^2. The magnitude of these parameters are physically meaningful. However, a discussion on the evaluation of these parameters as a function of exposure time will not be discussed.

The fitted resistance values of the organic coating (R_1) and resistance values of the interface and oxide layer (R_2) as a function of electrolyte exposure time are plotted in Fig. 14. The organic coating resistance R_1 shows a strong decreasing trend up till approximately 800 min after which a stable but low resistance value is reached. The decrease in R_1 resistance is explained by the diffusion of the borate buffer into the organic film. Due to electrolyte uptake, the conductivity of the organic film increases upon diffusion up till the point that the polymer is saturated by the electrolyte. The resistance (R_2) assigned to the interface and oxide behavior as a function of exposure time follows an increasing trend during the borate buffer exposure up till the polymer film is saturated by the electrolyte. The relatively

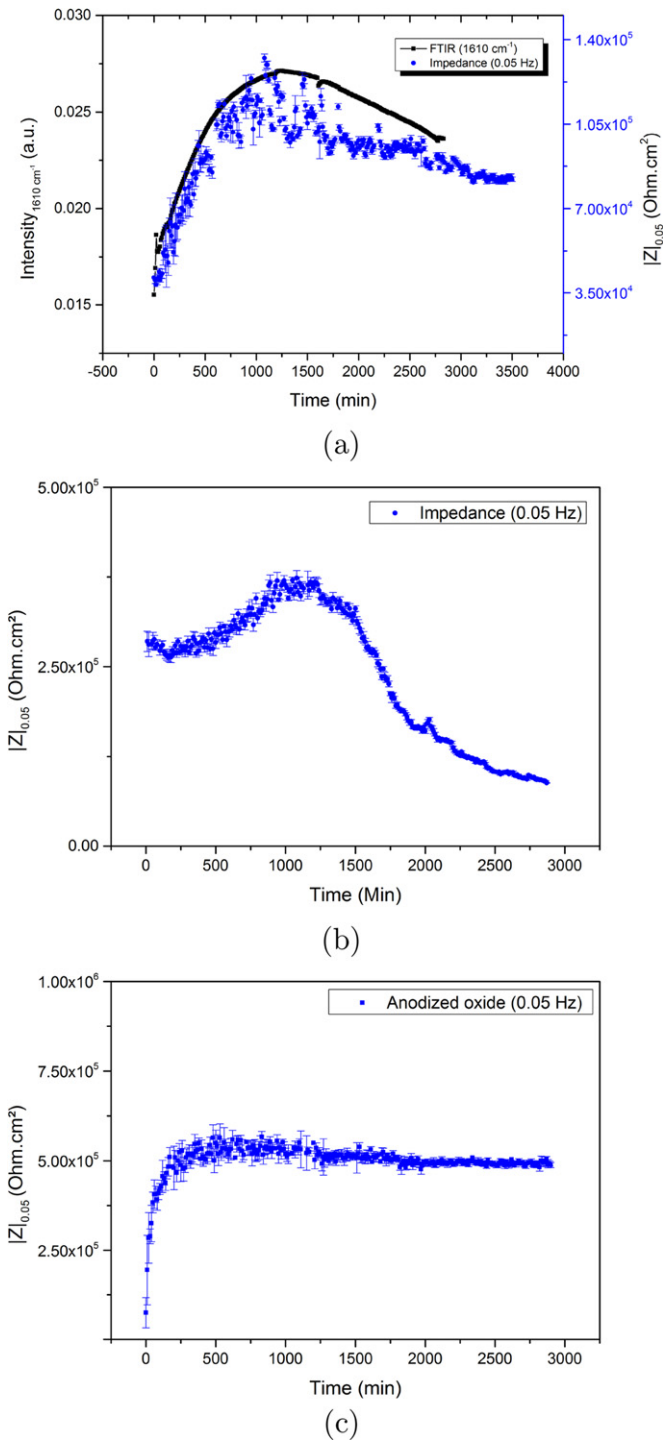

Fig. 11. Magnitude and error values of the impedance at 0.05 Hz (blue dots) for PAA deposited onto (a) *PVD aluminum oxide* obtained with the spectro-electrochemical setup, (b) *native aluminum oxide* and (c) *anodized aluminum oxide* as a function of electrolyte exposure.

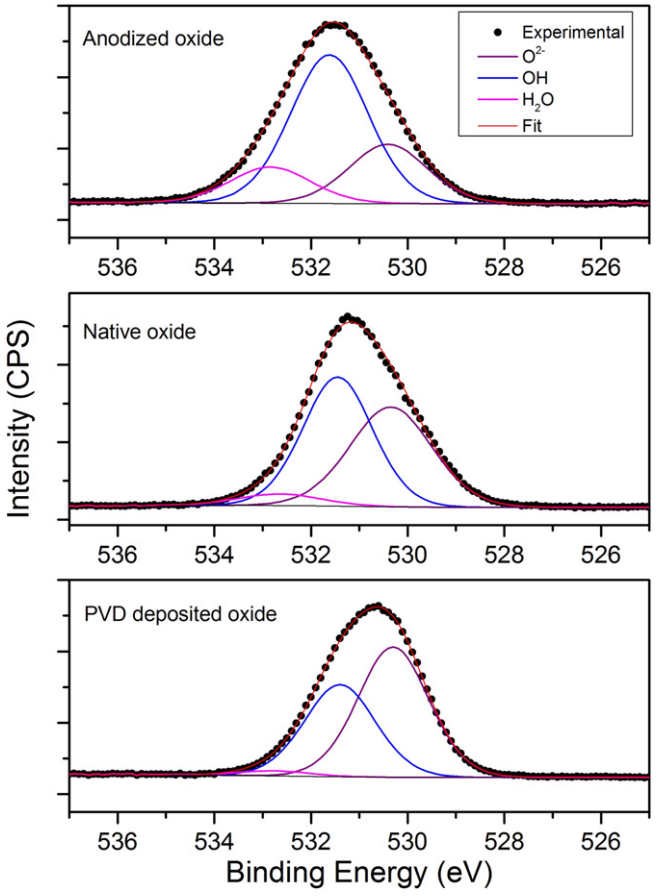

Fig. 12. O 1s XPS spectra for non-coated *PVD* deposited, *native* and *anodized aluminum oxide*. The O 1s spectra are fitted with an O^{2-} peak (purple), an OH peak (blue) and an adsorbed H_2O peak (pink).

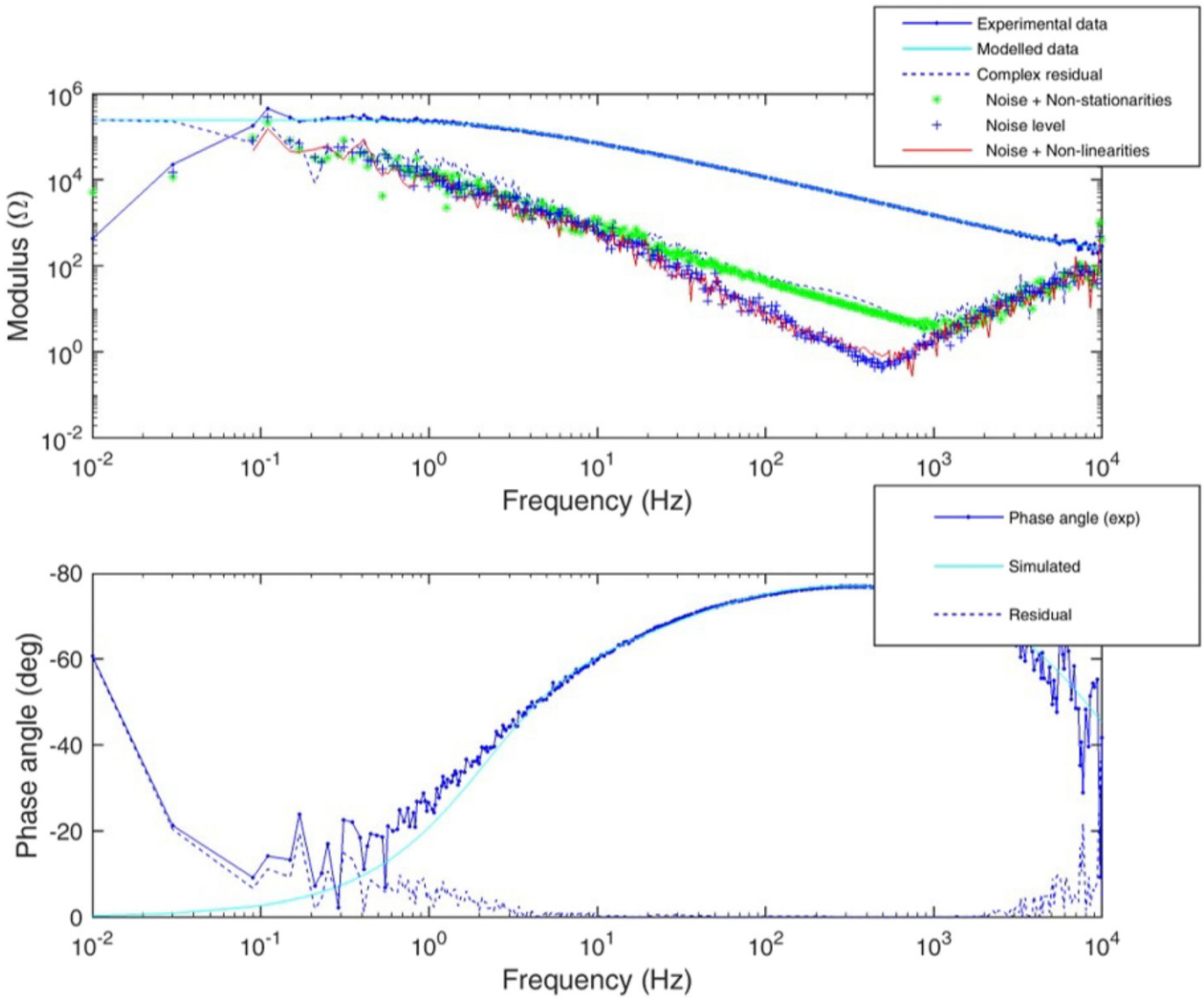

Fig. 13. Bode magnitude and phase plot containing the experimental data, modelled curve, complex residual, noise levels, noise on the excited frequencies and noise on the non-excited frequencies of the measurement at 1 h of exposure to the electrolyte of PMMA deposited on native aluminum oxide. Data is fitted with the same EEC as proposed in Fig. 7a.

larger error bars are a result of the low signal-to-noise ratio in the low frequency range during the diffusion of water. Afterwards, this signal-to-noise ratio of the measurement cycle increases in the low frequency region, leading to much smaller error bars. After the electrolyte diffusion, a plateau region in the resistance is reached. Also here, it is concluded that all three conditions for validity are met and that the proposed model is conclusive to describe borate buffer exposure to the PMMA/aluminum oxide system.

In Fig. 15, an overlay of the fitted R_2 resistance values of the PMMA/native aluminum oxide system is compared with the peak intensity of the carboxylate stretch ($1540\,cm^{-1}$) obtained with IR in the Kretschmann geometry of a PMMA/PVD deposited aluminum oxide. A good correlation is observed between the IR data of the ionic bond at the interface and the fitted R_2 values. Initially, an increase in ionic bond intensity/resistance value is followed by a plateau, suggesting no delamination of the PMMA from the aluminum oxide surface occurred.

4. Conclusion

The investigation reported here demonstrates the *in situ* monitoring of the aqueous effect on polymer/metal oxide interfaces. This is achieved by a spectro-electrochemical setup of FTIR in the Kretschmann geometry and odd random phase multisine electrochemical impedance spectroscopy. Since both techniques record data in the same time-frame, the obtained data can be directly compared. The interfacial interactions of ultrathin PAA depositions on an aluminum oxide surface are characterized as carboxylate ionic bonds and changes induced by the effect of water diffusion at the interface are probed *in situ*. This allowed to observe an initial increase in the amount of ionic bonds. However, after a certain exposure time the interfacial interactions are destroyed, which eventually leads to macroscopic delamination as shown by SEM images of pristine and electrolyte-exposed surfaces. The influence of the oxide type on the polymer/metal oxide interface is investigated and the stability of the

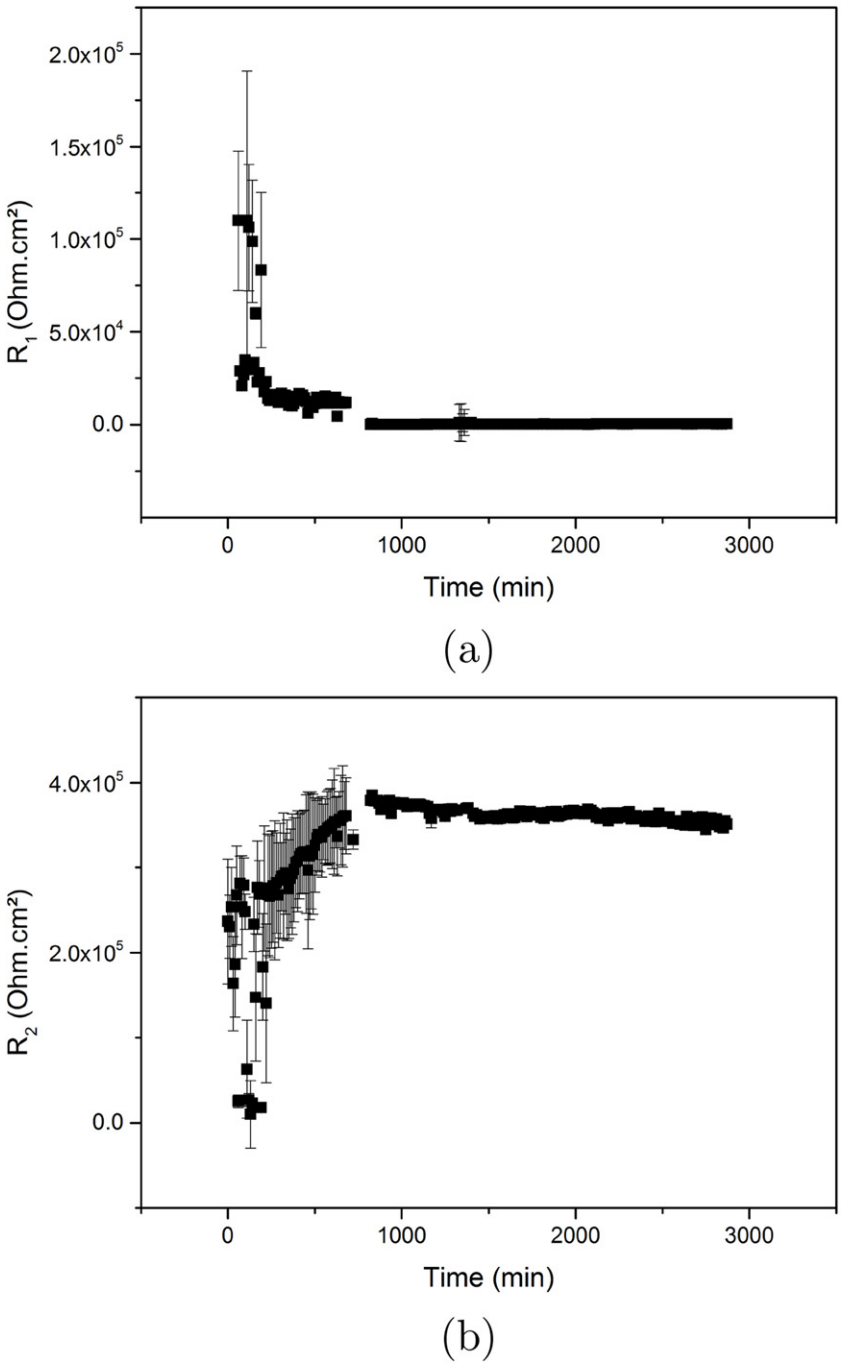

Fig. 14. Fitted resistance values with the EEC shown in Fig. 7a. Resistance values of the organic coating (R_1) and resistance values of the interface and oxide layer (R_2) as a function of electrolyte exposure time.

interfacial bonds is linked to the amount of free hydroxyl groups on the aluminum oxide surface. XPS spectra of anodized aluminum oxide showed a higher amount of hydroxyl groups than the *native* and *PVD aluminum oxide* and this could be linked to the impedance response of the low frequency region of PAA coated/*anodized aluminum oxide*, that showed a stable interface during the recorded electrolyte exposure time. An electric equivalent circuit was proposed to model the ORP EIS response of the PAA/aluminum oxide system and the fitted resistance values could be physically described. Finally, a PMMA deposition on aluminum oxide is investigated. PMMA contains a methyl methacrylate repeating unit and previous work showed that PMMA needs more water molecules at its interface to hydrolyse the methoxide group and to form a carboxylate bond with the metal oxide substrate. After fitting the proposed EEC, a correlation is observed between the fitted electrochemical parameter assigned to the interface and oxide layer and the IR peak of the asymmetric carboxylate stretch. Also for this system, an initial increase in the amount of bonds at the interface and the fitted resistance value is observed after which a stable region follows. This indicates that the PMMA/*native aluminum oxide* forms a more stable interface than the PAA/*native aluminum oxide*. This difference in stability might be explained due to the different adsorption

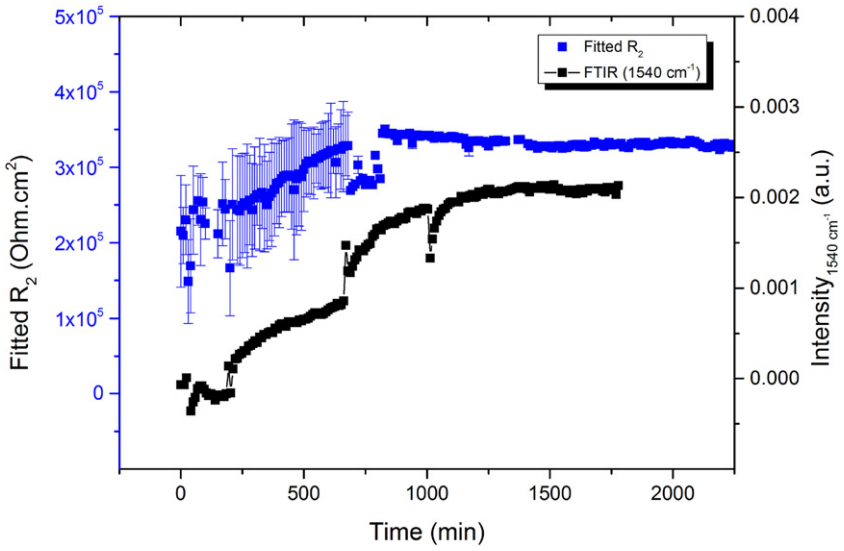

Fig. 15. Overlay of FTIR and Impedance data. The intensity of the asymmetric $\nu_{as}(COO^-)$ carboxylate stretch located at 1540 cm^{-1} and baseline corrected as a function of electrolyte exposure time (black dotted line) obtained with FTIR in the Kretschmann geometry; Magnitude and error values of the fitted R_2 resistance (blue dots) of PMMA deposited on native aluminum oxide. A direct link is observed between the carboxylate bond at the interface and the fitted R_2 resistance.

mechanisms of the respective polymers to bond to the aluminum oxide surface. For PMMA, the adsorption mechanism of the polymer on the aluminum oxide surface showed the need of a hydrolysis step, followed by a deprotonation step [7]. This means that more water is consumed at the interface to form the carboxylate bond, than is the case for PAA. For PAA, the thermodynamic equilibrium at the interface is shifted much faster towards bond breakage than for PMMA [10, 11]. However, after continuous diffusion of the water molecules, eventually also the thermodynamic equilibrium will shift at the PMMA/aluminum oxide interface and prolonged exposure time will also lead to bond breakage of the ionic bond. These observations show that IR spectroscopy in the Kretschmann geometry and ORP EIS are suited techniques to *in situ* monitor interfacial interactions at polymer/metal oxide systems under aqueous conditions. It can be concluded that both the surface properties of the metal oxide as well as functional groups of the polymer can alter the stability of their interface when exposed to aqueous conditions.

Declaration of Competing Interest

None.

Acknowledgements

S.P., H.T. and T.H. acknowledge financial support by Research Foundation - Flanders (FWO) under project number SB-19-151.

References

[1] S. Lyon, R. Bingham, D. Mills, Advances in corrosion protection by organic coatings: what we know and what we would like to know, Prog. Org. Coat. 102 (2017) 2–7. https://doi.org/10.1016/j.porgcoat.2016.04.030.
[2] P. Taheri, J.R. Flores, F. Hannour, J. H. W. de Wit, H. Terryn, J.M.C. Mol, In situ study of buried interfacial bonding mechanisms of carboxylic polymers on Zn surfaces, J. Phys. Chem. C 117 (7) (2013) 3374–3382. https://doi.org/10.1021/jp310813g.
[3] G. Grundmeier, M. Stratmann, Adhesion and de-adhesion mechanisms at polymer/metal interfaces: mechanistic understanding based on in situ studies of buried interfaces, Annu. Rev. Mater. Res. 35 (1) (2005) 571–615. https://doi.org/10.1146/annurev.matsci.34.012703.105111.
[4] S. Pletincx, S. Abrahami, J.M.C. Mol, T. Hauffman, H. Terryn, Advanced (in situ) surface analysis of organic coating/metal oxide interactions for corrosion protection of passivated metals, Encyclopedia of Interfacial Chemistry, Elsevier. 2018, pp. 1–17. https://doi.org/10.1016/B978-0-12-409547-2.13773-4.
[5] A. González-Orive, I. Giner, T. de los Arcos, A. Keller, G. Grundmeier, Analysis of polymer/oxide interfaces under ambient conditions: an experimental perspective, Appl. Surf. Sci. 442 (2018) 581–594. https://doi.org/10.1016/j.apsusc.2018.02.155.
[6] S. Pletincx, L.L.I. Fockaert, J.M.C. Mol, T. Hauffman, H. Terryn, Probing the formation and degradation of chemical interactions from model molecule/metal oxide to buried polymer/metal oxide interfaces, npj Materials Degradation 3 (1) (2019) 23. https://doi.org/10.1038/s41529-019-0085-2.
[7] S. Pletincx, K. Marcoen, L. Trotochaud, L.L.I. Fockaert, J.M.C. Mol, A.R. Head, O. Karslıoğlu, H. Bluhm, H. Terryn, T. Hauffman, Unravelling the chemical influence of water on the PMMA/aluminum oxide hybrid interface in situ, Sci. Rep. 7 (1) (2017) 13341. https://doi.org/10.1038/s41598-017-13549-z.
[8] S. Pletincx, L. Trotochaud, L.L.I. Fockaert, J.M.C. Mol, A.R. Head, O. Karslıoğlu, H. Bluhm, H. Terryn, T. Hauffman, In Situ Characterization of the initial effect of water on molecular interactions at the interface of organic/inorganic hybrid systems, Sci. Rep. 7 (45123) (2017) 45123. https://doi.org/10.1038/srep45123.
[9] J.F. Watts, M.M. Chehimi, E.M. Gibson, Acid-base interactions in adhesion: the characterization of surfaces & interfaces by XPS, J. Adhes. 39 (2-3) (1992) 145–156. https://doi.org/10.1080/00218469208026546.
[10] R. Tannenbaum, S. King, J. Lecy, M. Tirrell, L. Potts, Infrared study of the kinetics and mechanism of adsorption of acrylic polymers on alumina surfaces, Langmuir 20 (18) (2004) 4507–4514. https://doi.org/10.1021/la036137v.
[11] K. Konstadinidis, B. Thakkar, a. Chakraborty, L.W. Potts, R. Tannenbaum, M. Tirrell, J.F. Evans, Segment level chemistry and chain conformation in the reactive adsorption of poly(methyl methacrylate) on aluminum oxide surfaces, Langmuir 8 (5) (1992) 1307–1317. https://doi.org/10.1021/la00041a012.
[12] S. Leadley, J. Watts, The use of XPS to examine the interaction of poly(acrylic acid) with oxidised metal substrates, J. Electron Spectrosc. Relat. Phenom. 85 (1-2) (1997) 107–121. https://doi.org/10.1016/S0368-2048(97)00028-5.
[13] S.R. Leadley, J.F. Watts, The use of XPS to examine the interaction of PMMA with oxidised metal substrates, J. Electron Spectrosc. Relat. Phenom. 85 (12) (1997) 107–121. https://doi.org/10.1016/S0368-2048(97)00028-5.
[14] M. Stratmann, A. Leng, W. Fürbeth, H. Streckel, H. Gehmecker, K.H. Große-Brinkhaus, The scanning Kelvin probe; a new technique for the in situ analysis of the delamination of organic coatings, Prog. Org. Coat. 27 (1-4) (1996) 261–267. https://doi.org/10.1016/0300-9440(94)00542-7.
[15] A. Leng, H. Streckel, M. Stratmann, The delamination of polymeric coatings from steel. Part 1: calibration of the Kelvin probe and basic delamination mechanism, Corros. Sci. 41 (3) (1998) 547–578. https://doi.org/10.1016/S0010-938X(98)00166-8.
[16] A. Leng, H. Streckel, M. Stratmann, The delamination of polymeric coatings from steel. Part 2: first stage of delamination, effect of type and concentration of cations on delamination, chemical analysis of the interface, Corros. Sci. 41 (3) (1998) 579–597. https://doi.org/10.1016/S0010-938X(98)00167-X.
[17] A. Leng, H. Streckel, K. Hofmann, M. Stratmann, The delamination of polymeric coatings from steel Part 3: effect of the oxygen partial pressure on the delamination reaction and current distribution at the metal/polymer interface, Corros. Sci. 41 (3) (1998) 599–620. https://doi.org/10.1016/S0010-938X(98)00168-1.

[18] W. Fürbeth, M. Stratmann, Delamination of polymeric coatings from electrogalvanized steel — a mechanistic approach. Part 1: delamination from a defect with intact zinc layer, Corros. Sci. 43 (2) (2001) 207–227. https://doi.org/10.1016/S0010-938X(00)00047-0.
[19] D. Vijayshankar, A. Altin, C. Merola, A. Bashir, E. Heinen, M. Rohwerder, Probing the buried metal-organic coating interfacial reaction kinetic mechanisms by a hydrogen permeation based potentiometric approach, J. Electrochem. Soc. 163 (13) (2016) C778–C783. https://doi.org/10.1149/2.0971613jes.
[20] A.S. Castela, A.M. Simoes, An impedance model for the estimation of water absorption in organic coatings. Part I: a linear dielectric mixture equation, Corros. Sci. 45 (8) (2003) 1631–1646. https://doi.org/10.1016/S0010-938X(03)00014-3.
[21] J.T. Zhang, J.M. Hu, J.Q. Zhang, C.N. Cao, Studies of water transport behavior and impedance models of epoxy-coated metals in NaCl solution by EIS, Prog. Org. Coat. 51 (2) (2004) 145–151. https://doi.org/10.1016/j.porgcoat.2004.08.001.
[22] T. Nguyen, E. Byrd, D. Bentz, Quantifying water at the organic film/hydroxylated substrate interface, J. Adhes. 48 (1-4) (1995) 169–194. https://doi.org/10.1080/00218469508028161.
[23] I. Linossier, F. Gaillard, M. Romand, T. Nguyen, A spectroscopic technique for studies of water transport along the interface and hydrolytic stability of polymer/substrate systems, J. Adhes. 70 (3-4) (1999) 221–239. https://doi.org/10.1080/00218469908009557.
[24] L. Philippe, C. Sammon, S.B. Lyon, J. Yarwood, An FTIR/ATR in situ study of sorption and transport in corrosion protective organic coatings: paper 2. The effects of temperature and isotopic dilution, Prog. Org. Coat. 49 (4) (2004) 315–323. https://doi.org/10.1016/j.porgcoat.2003.10.007.
[25] F. Mansfeld, S. Jeanjaquet, M. Kendig, An electrochemical impedance spectroscopy study of reactions at the metal/coating interface, Corros. Sci. 26 (9) (1986) 735–742. https://doi.org/10.1016/0010-938X(86)90037-5.
[26] A. Amirudin, D. Thieny, Application of electrochemical impedance spectroscopy to study the degradation of polymer-coated metals, Prog. Org. Coat. 26 (1) (1995) 1–28. https://doi.org/10.1016/0300-9440(95)00581-1.
[27] F. Deflorian, L. Fedrizzi, Adhesion characterization of protective organic coatings by electrochemical impedance spectroscopy, J. Adhes. Sci. Technol. 13 (5) (1999) 629–645. https://doi.org/10.1163/156856199X00154.
[28] R. Vlasak, I. Klueppel, G. Grundmeier, Combined EIS and FTIR-ATR study of water uptake and diffusion in polymer films on semiconducting electrodes, Electrochim. Acta 52 (28) (2007) 8075–8080. https://doi.org/10.1016/j.electacta.2007.07.003.
[29] M. Öhman, D. Persson, An integrated in situ ATR-FTIR and EIS set-up to study buried metal-polymer interfaces exposed to an electrolyte solution, Electrochim. Acta 52 (16) (2007) 5159–5171. https://doi.org/10.1016/j.electacta.2007.02.007.
[30] M. Öhman, Development of ATR-FTIR Kretschmann Spectroscopy for In situ Studies of Metal/Polymer Interfaces and its Integration with EIS for Exposure to Corrosive Conditions, 2010.
[31] M. Öhman, D. Persson, ATR-FTIR Kretschmann spectroscopy for interfacial studies of a hidden aluminum surface coated with a silane film and epoxy I. Characterization by IRRAS and ATR-FTIR, Surf. Interface Anal. 44 (2) (2012) 133–143. https://doi.org/10.1002/sia.3779.
[32] S. Pletincx, L.L.I. Fockaert, M. Meeusen, J.M.C. Mol, H. Terryn, T. Hauffman, In situ methanol adsorption on aluminum oxide monitored by a combined ORP-EIS and ATR-FTIR Kretschmann setup, J. Phys. Chem. C 122 (38) (2018) 21963–21973. https://doi.org/10.1021/acs.jpcc.8b06806.
[33] M. Öhman, D. Persson, D. Jacobsson, In situ studies of conversion coated zinc/polymer surfaces during exposure to corrosive conditions, Prog. Org. Coat. 70 (2011) 16–22. https://doi.org/10.1016/j.porgcoat.2010.09.012.
[34] Y. Van Ingelgem, E. Tourwé, O. Blajiev, R. Pintelon, A. Hubin, Advantages of odd random phase multisine electrochemical impedance measurements, Electroanalysis 21 (6) (2009) 730–739. https://doi.org/10.1002/elan.200804471.
[35] E. Van Gheem, R. Pintelon, J. Vereecken, J. Schoukens, A. Hubin, P. Verboven, O. Blajiev, Electrochemical impedance spectroscopy in the presence of non-linear distortions and non-stationary behaviour Part I: theory and validation, Electrochim. Acta 49 (26) (2004) 4753–4762. https://doi.org/10.1016/j.electacta.2004.05.039.
[36] T. Breugelmans, E. Tourwé, J.B. Jorcin, A. Alvarez-Pampliega, B. Geboes, H. Terryn, A. Hubin, Odd random phase multisine EIS for organic coating analysis, Prog. Org. Coat. 69 (2) (2010) 215–218. https://doi.org/10.1016/j.porgcoat.2010.04.008.
[37] T. Hauffman, Y. Van Ingelgem, T. Breugelmans, E. Tourwé, H. Terryn, A. Hubin, Dynamic, in situ study of self-assembling organic phosphonic acid monolayers from ethanolic solutions on aluminium oxides by means of odd random phase multisine electrochemical impedance spectroscopy, Electrochim. Acta 106 (2013) 342–350. https://doi.org/10.1016/j.electacta.2013.04.025.
[38] R. Messier, A.P. Giri, R.A. Roy, Revised structure zone model for thin film physical structure, J. Vac. Sci. Technol. A 2 (2) (2002) 500–503. https://doi.org/10.1116/1.572604.
[39] J. Schoukens, R. Pintelon, E.V. Der Ouderaa, J. Renneboog, Survey of excitation signals for FFT based signal analyzers, IEEE Trans. Instrum. Meas. 37 (3) (1988) 342–352. https://doi.org/10.1109/19.7453.
[40] J. Schoukens, R. Pintelon, T. Dobrowiecki, Linear modeling in the presence of nonlinear distortions, IEEE Trans. Instrum. Meas. 51 (4) (2002) 786–792. https://doi.org/10.1109/TIM.2002.803298.
[41] L. Fernández Macía, M. Petrova, T. Hauffman, T. Muselle, T. Doneux, A. Hubin, A study of the electron transfer inhibition on a charged self-assembled monolayer modified gold electrode by odd random phase multisine electrochemical impedance spectroscopy, Electrochim. Acta 140 (2014) 282–293. https://doi.org/10.1016/j.electacta.2014.05.027.
[42] E. Koo, S. Yoon, S. V. Atre, D. L. Allara, Robust, functionalizable, nanometer-thick poly(acrylic acid) films spontaneously assembled on oxidized aluminum substrates: structures and chemical properties, Langmuir, 10.1021/la104840c.
[43] J. Evertsson, F. Bertram, F. Zhang, L. Rullik, L.R. Merte, M. Shipilin, M. Soldemo, S. Ahmadi, N. Vinogradov, F. Carlà, J. Weissenrieder, M. Göthelid, J. Pan, A. Mikkelsen, J.O. Nilsson, E. Lundgren, The thickness of native oxides on aluminum alloys and single crystals, Appl. Surf. Sci. 349 (2015) 826–832. https://doi.org/10.1016/j.apsusc.2015.05.043.
[44] M.R. Alexander, G.E. Thompson, G. Beamson, Characterization of the oxide/hydroxide surface of aluminum using X-ray photoelectron spectroscopy: a procedure for curve fitting the O 1s core level, Surf. Interface Anal. 29 (7) (2000) 468–477. https://doi.org/10.1002/1096-9918(200007)29:7¡468::AID-SIA890¿3.0.CO;2\ignorespaces-V.
[45] T. Hauffman, A. Hubin, H. Terryn, Study of the self-assembling of *n*-octylphosphonic acid layers on aluminum oxide from ethanolic solutions, Surf. Interface Anal. 45 (10) (2013) 1435–1440. https://doi.org/10.1002/sia.5150.
[46] J. Wielant, T. Hauffman, O. Blajiev, R. Hausbrand, H. Terryn, Influence of the iron oxide acid-base properties on the chemisorption of model epoxy compounds studied by XPS, J. Phys. Chem. C 111 (35) (2007) 13177–13184.
[47] J. Van Den Brand, On the Adhesion Between Aluminium and Polymers, PhD thesis, TU Delft, 2004.
[48] O.O. Blajiev, A. Ithurbide, A. Hubin, C. Van Haesendonck, H. Terryn, XPS study of the assembling morphology of 3-hydroxy-3-phosphono-butiric acid tert-butyl ester on variously pretreated Al surfaces, Prog. Org. Coat. 63 (3) (2008) 272–281. https://doi.org/10.1016/j.porgcoat.2007.11.007.
[49] P. Taheri, T. Hauffman, J.M.C. Mol, J.R. Flores, F. Hannour, J. H. W. de Wit, H. Terryn, Molecular interactions of electroadsorbed carboxylic acid and succinic anhydride monomers on zinc surfaces, J. Phys. Chem. C 115 (34) (2011) 17054–17067. https://doi.org/10.1021/jp204751z.
[50] P. Taheri, K. Pohl, G. Grundmeier, J.R. Flores, F. Hannour, J.H. De Wit, J.M. Mol, H. Terryn, Effects of surface treatment and carboxylic acid and anhydride molecular dipole moments on the Volta potential values of zinc surfaces, J. Phys. Chem. C 117 (4) (2013) 1712–1721. https://doi.org/10.1021/jp3096049.
[51] S.T. Abrahami, J. M. M. de Kok, V.C. Gudla, R. Ambat, H. Terryn, J.M.C. Mol, Interface strength and degradation of adhesively bonded porous aluminum oxides, npj Materials Degradation 1 (1) (2017) 8. https://doi.org/10.1038/s41529-017-0007-0.
[52] S. Tardio, M.L. Abel, R.H. Carr, J.F. Watts, The interfacial interaction between isocyanate and stainless steel, Int. J. Adhes. Adhes. 88 (2019) 1–10. https://doi.org/10.1016/j.ijadhadh.2018.10.008.